J Physiol 592.21 (2014) pp 4747–4762

The Journal of Physiology

Angiotensin II mobilizes intracellular calcium and activates pannexin-1 channels in rat carotid body type II cells via AT_1 receptors

Sindhubarathi Murali, Min Zhang and Colin A. Nurse

Department of Biology, McMaster University, 1280 Main St West, Hamilton, Ontario, Canada, L8S 4K1

Key points

- A locally generating, angiotensin II (ANG II) system is present in the rat carotid body (CB) and up-regulation of this system occurs in certain pathophysiological situations, enhancing sympathetic activity.
- Here, we show that, similar to chemoreceptor type I cells, glial-like type II cells also express functional AT_1Rs, stimulation of which causes release of Ca^{2+} from intracellular stores.
- ANG II–AT_1R signalling in type II cells activates an inward current carried by pannexin-1 (Panx-1) channels which are known to act as conduits for release of ATP, a key CB excitatory neurotransmitter.
- Combined effects of ANG II and ATP, which also activates Panx-1 currents via P2Y2 receptors, were synergistic; chelating intracellular Ca^{2+} with BAPTA prevented Panx-1 current activation.
- We propose that the excitatory function of ANG II in the CB involves dual actions at both type I and type II cells.

Abstract A local angiotensin-generating system is present in the carotid body (CB) and increased angiotensin II (ANG II) signalling contributes to enhanced CB excitation in chronic heart failure (CHF) and after chronic or intermittent hypoxia. ANG II actions have thus far been attributed solely to stimulation of AT_1 receptors (AT_1Rs) on chemoreceptor type I cells. Here, we show that in dissociated rat CB cultures, ANG II also stimulates glial-like type II cells, identified by P2Y2-receptor-induced intracellular Ca^{2+} elevation ($\Delta[Ca^{2+}]_i$). ANG II induced a dose-dependent (EC_{50} ~8 nM), robust $\Delta[Ca^{2+}]_i$ in type II cells that was reversibly abolished by the AT_1R blocker losartan (1 μM). The ANG II-induced $\Delta[Ca^{2+}]_i$ persisted in Ca^{2+}-free medium but was sensitive to store depletion with cyclopiazonic acid (1 μM). Similar to P2Y2 receptor agonists, ANG II (20–1000 nM) activated pannexin-1 (Panx-1) current that was reversibly abolished by carbenoxolone (5 μM). This current arose with a variable delay and was reversibly inhibited by losartan. Repeated application of ANG II often led to current run-down, attributable to AT_1R desensitization. When applied to the same cell the combined actions of ANG II and ATP on Panx-1 current were synergistic. Current induced by either ligand was inhibited by BAPTA-AM (1 μM), suggesting that intracellular Ca^{2+} signalling contributed to Panx-1 channel activation. Because open Panx-1 channels release ATP, a key CB excitatory neurotransmitter, it is plausible that paracrine stimulation of type II cells by ANG II contributes to enhanced CB excitability, especially in pathophysiological conditions such as CHF and sleep apnoea.

DOI: 10.1113/jphysiol.2014.279299

(Received 13 June 2014; accepted after revision 14 August 2014; first published online 28 August 2014)
Corresponding author C. A. Nurse: Department of Biology, McMaster University, 1280 Main Street West, Hamilton, Ontario, Canada, L8S 4K1. Email: nursec@mcmaster.ca

Abbreviations ANG II, angiotensin II; AT_1R, AT_1 receptor; CB, carotid body; CBX, carbenoxolone; CHF, chronic heart failure; IP_3, inositol-1,4,5-trisphosphate; Panx-1, pannexin-1; P2Y2R, P2Y2 receptor; RAS, renin–angiotensin system.

Introduction

The chemosensory carotid body (CB) plays an important role in the reflex control of ventilation, as well as in the autonomic control of cardiovascular functions (Kumar & Prabhakar, 2012). CB stimulation during hypoxaemia enhances cardiovascular performance and protects vital organs via an increase in sympathetic efferent activity and circulatory levels of vasoactive hormones including the octapeptide, angiotensin II (ANG II) (Marshall, 1994). ANG II is a key component of the renin–angiotensin system (RAS) that is involved in blood pressure regulation and fluid homeostasis. Interestingly, however, a locally generating, renin-independent RAS system has been described in the CB (Lam & Leung, 2002), and hyperactivity within this system is associated with several pathophysiological conditions such as chronic heart failure (CHF) and exposures to chronic and intermittent hypoxia (Schultz, 2011; Kumar & Prabhakar, 2012). Indeed, both systemic and tissue RAS are activated during hypoxia, leading to an increase in plasma ANG II (Zakheim *et al.* 1976), and infusion of exogenous ANG II in the peripheral circulation stimulates cardiorespiratory functions (Ohtake & Jennings, 1993; Li *et al.* 2006). Moreover, superfusion of the isolated rat CB with ANG II *in vitro* increases afferent nerve discharge (Allen, 1998), and perfusion of the vascularly isolated rabbit carotid sinus region with ANG II augments the hypoxia-evoked CB chemoreceptor discharge (Li *et al.* 2006). Taken together, these studies indicate that ANG II signalling pathways play an important excitatory role in CB function.

Studies on the role of ANG II in the CB have so far focused on the chemoreceptor type I cells. Autoradiographic studies have revealed a high density of angiotensin AT_1 receptors (AT_1Rs) over type I cell clusters of the rat CB (Allen, 1998), and both angiotensin-converting enzyme (ACE) and angiotensinogen (the precursor of ANG II) are expressed in type I cells (Leung *et al.* 2000; Lam & Leung, 2003). While the role of endogenous ANG II in the normal CB function remains unclear (Li *et al.* 2006), there is functional evidence that exogenous ANG II causes a concentration-dependent increase in intracellular Ca^{2+} in isolated rat type I cells via losartan-sensitive AT_1Rs (Fung *et al.* 2001). Also, transcripts for both A- and B-isoforms of AT_1Rs have been detected by RT-PCR in whole rat CB and there is immunohistochemical evidence for AT_1R protein expression in type I cells of rat and rabbit CB (Fung *et al.* 2001; Li *et al.* 2006). Importantly, components of the local RAS system in the CB are regulated by different patterns of hypoxia exposure, and the type I cells seem to be a major target (Leung *et al.* 2000; Lam *et al.* 2014). For example, in a recent study, exposure to chronic intermittent hypoxia led to upregulation of RAS components in the rat CB, in association with enhanced type I cell intracellular Ca^{2+} responses to exogenous ANG II (Lam *et al.* 2014).

Recent evidence from this laboratory suggests that sensory processing in the rat CB may involve not only the chemoreceptor type I cells, which release the excitatory neurotransmitter ATP, but also adjacent sustentacular, 'glial-like' type II cells (Nurse, 2010; Nurse & Piskuric, 2012; Zhang *et al.* 2012). It was proposed that during chemotransduction paracrine stimulation of P2Y2 receptors (P2Y2Rs) on type II cells may help boost the ATP signal, and therefore CB excitation, by activating pannexin-1 (Panx-1) channels which act as conduits for ATP release (Zhang *et al.* 2012). P2Y2R stimulation leads to a rise in intracellular Ca^{2+} in type II cells (Xu *et al.* 2003; Zhang *et al.* 2012), and this is thought to be a trigger for Panx-1 channel opening. Interestingly, it was briefly noted in a recent review that type II cells may also respond to ANG II with a rise in intracellular Ca^{2+} (Tse *et al.* 2012), raising the possibility that ANG II actions in the CB may be more complex than initially thought. In the present study we extend this initial observation and show that ANG II, acting via AT_1Rs in type II cells, induces a robust increase in intracellular Ca^{2+}, which in turn leads to Panx-1 channel activation. These data strongly suggest that the excitatory role of ANG II in the CB probably involves dual actions at both type I and type II cells.

Methods

Ethical approval

All procedures for animal handling and tissue dissections were carried out according to the guidelines of the Canadian Council on Animal Care (CCAC) and institutional guidelines. The authors have read, and the experiments comply with, the policies and regulations of *The Journal of Physiology* as stated by Drummond (2009).

Cell cultures of dissociated rat carotid body

Carotid bifurcations from 9- to 14-day-old rats (Wistar, Charles River, Quebec, Canada) were excised bilaterally, after the animals were first rendered unconscious by a blow to the back of the head, followed immediately by decapitation. The carotid bodies (CBs) were isolated from the surrounding tissue and dissociated cell cultures prepared according to established procedures, described in detail elsewhere (Zhong *et al.* 1997; Zhang *et al.* 2000). Briefly, the excised CBs were incubated for 1 h at 37°C in a physiological salt solution containing 0.1% trypsin (Sigma-Aldrich, Oakville, Ontario, Canada) and 0.1% collagenase (Gibco, Grand Island, NY, USA), followed by mechanical dissociation and trituration. The dispersed cell suspension was allowed to adhere to the central wells of modified tissue culture dishes; the wells were pre-coated with a thin layer of Matrigel (BD Biosciences, Mississauga, Ontario, Canada). The cells were cultured in basic growth medium (BGM) consisting of F-12 nutrient medium supplemented with 10% fetal bovine serum, 1% penicillin–streptomycin, 1% glutamine, 0.3% glucose and 3 μg ml^{-1} insulin, as in previous studies (Zhang *et al.* 2000, 2012). To enrich for type II cells and facilitate recordings, the growth medium was switched after 12 h to Cosmic-BGM containing: 50% BGM plus 50% of modified BGM where 10% fetal bovine serum was replaced with 5% fetal bovine serum and 5% Cosmic calf serum (Hyclone Laboratories Inc., Logan, UT, USA). Our previous study demonstrated that there were no obvious differences in the properties of type II cells cultured in BGM *versus* Cosmic-BGM (Zhang *et al.* 2012). In some experiments, phorbol 12-myristate 13-acetate (PMA; 100 nM) was added to the culture medium in an attempt to minimize AT_1 receptor desensitization (Zhang *et al.* 1996). Cultures were grown at 37°C in a humidified atmosphere of 95% air–5% CO_2. Patch clamp recordings were usually carried out in 5- to 7-day-old CB cultures, which permitted optimal recordings from isolated 'solitary' type II cells; the Ca^{2+} imaging experiments were typically carried out after ~48 h in culture.

Intracellular Ca^{2+} measurements

Intracellular free Ca^{2+} concentration ($[Ca^{2+}]_i$) was monitored using the acetoxymethyl ester (AM) form of the fluorescent Ca^{2+} indicator fura-2 (fura-2 AM; Molecular Probes, Eugene, OR, USA), as previously described (Piskuric & Nurse, 2012; Zhang *et al.* 2012). Cells were loaded with 2.5 μM fura-2 AM diluted in standard bicarbonate-buffered solution (BBS) for 30 min at 37°C, and subsequently washed for ~15 min to remove free dye. The BBS used in Ca^{2+} imaging experiments had the following composition (in mM): $NaHCO_3$, 24; NaCl, 115; glucose, 5; KCl, 5; $CaCl_2$, 2 and $MgCl_2$, 1; the pH was maintained at ~7.4 by bubbling with a 5% CO_2–95% air mixture. Ratiometric Ca^{2+} imaging was performed using a Nikon Eclipse TE2000-U inverted microscope (Nikon, Mississauga, ON, Canada) equipped with a Lambda DG-4 ultra-high-speed wavelength changer (Sutter Instrument Co., Novato, CA, USA), a Hamamatsu OCRCA-ET digital CCD camera (Hamamatsu, Sewickley, PA, USA) and a Nikon S-Fluor ×40 oil-immersion objective lens with a numerical aperture of 1.3. Dual images at 340 nm and 380 nm excitation (510 nm emission) were acquired every 2 s, with an exposure time of 100–200 ms. Pseudocolour ratiometric data were obtained using Simple PCI software version 5.3. All experiments were performed at 35–37°C, and cells were continuously perfused with BBS to maintain an extracellular pH of ~7.4.

The imaging system was calibrated using the Fura-2 Calcium Imaging Calibration Kit from Molecular Probes (Cat. No. F-6774). Photometric data at 340 nm and 380 nm excitation (510 nm emission) were obtained for 11 buffers of known Ca^{2+} concentrations from Ca^{2+}-free (0 μM) to saturating Ca^{2+} (39 μM). After correcting for background fluorescence, these values were used to calculate the following ratios: 'R' is the ratio of 510 nm emission intensity at 340 nm excitation to 510 nm emission intensity at 380 nm excitation; R_{min} is the ratio at zero free Ca^{2+}; R_{max} is the ratio at saturating Ca^{2+}; and β, the fluorescence intensity with excitation at 380 nm for zero free Ca^{2+} (F_{380max}), to the fluorescence intensity at saturating free Ca^{2+} (F_{380min}). The intracellular free $[Ca^{2+}]$ was obtained after substituting these ratios into the Grynkiewicz equation (Grynkiewicz *et al.* 1985) as follows:

$$[Ca^{2+}]_i = K_d \frac{[R - R_{min}]}{[R_{max} - R]} \beta$$

where $R_{min} = 0.18$, $R_{max} = 7.81$, $\beta = 12.29$, $K_d = 225$ nM and R is the ratio obtained during the experiment for a given cell. For most experiments statistical analysis was performed using repeated measures ANOVA with Tukey's multiple comparison test *post hoc* test, as indicated in the text.

Electrophysiology

Nystatin perforated-patch whole cell-recording was used to monitor ionic currents in type II cells as previously described (Zhang *et al.* 2000, 2012). All recordings were carried out at ~35°C and the cells were perfused with standard BBS containing (in mM): $NaHCO_3$, 24; NaCl, 115; KCl, 5; $CaCl_2$, 2; $MgCl_2$, 1; glucose, 10; and sucrose, 12; at pH 7.4 maintained by bubbling with a 5% CO_2–95% air mixture. The pipette solution contained (mM): potassium gluconate, 115; KCl, 25; NaCl, 5; $CaCl_2$, 1; Hepes, 10; and nystatin, 200 μg ml^{-1}; at pH 7.2. Agonists (e.g. ANG II,

ATP) were applied by a 'fast perfusion' system utilizing a double-barrelled pipette assembly as previously described (Zhong *et al.* 1997: Zhang *et al.* 2000, 2012). Current measurements under voltage clamp were obtained with the aid of a MultiClamp 700A patch clamp amplifier and a Digidata 1322A analog-to-digital converter (Axon Instruments Inc., Union City, CA, USA), and the data stored on a personal computer. Data acquisition and analysis were performed using pCLAMP software (version 9.0; Axon Instruments Inc.). Because of the desensitization properties of the AT_1 receptor and long latency of the ANG II-induced current, we used a repeated ramp protocol to obtain an estimate of the reversal potential of $I_{ANG\,II}$. Starting with a holding potential of −60 mV, the voltage was ramped every 6 s from −40 to +20 mV over a period of 700 ms. The ramp protocol was first applied just before ANG II exposure (to obtain the control *I–V* plot) and then the cycle was repeated at 6 s intervals throughout the ANG II exposure period. The ANG II-induced *I–V* plot during the peak or plateau phase of the current was selected and then subtracted from the initial control plot so as to obtain the $I_{ANG\,II}$ difference current and an estimate of the reversal potential. For multiple comparisons of ionic currents or current density (pA/pF; obtained by dividing peak current by whole cell capacitance), ANOVA was used and the level of significance was set at $P < 0.05$.

Reagents and drugs

The following reagents and drugs were obtained from Sigma-Aldrich (Oakville, ON, Canada): ATP, UTP, angiotensin II (ANG II), losartan potassium and carbenoxolone (CBX).

Results

The majority of the experiments described below were carried out on isolated 'solitary' type II cells to eliminate or minimize secondary or indirect effects from neighbouring type I cells. Such effects may arise within type I cell clusters as a result of the known stimulatory actions of ANG II on type I cells (Fung *et al.* 2001; Schultz, 2011). A few experiments were done on type I cells, present within characteristic clusters that are readily identified in these cultures under phase contrast microscopy (Nurse, 2010). In Ca^{2+} imaging experiments, type II cells were routinely identified by the presence of a robust increase in intracellular Ca^{2+} ($\Delta[Ca^{2+}]_i$) during exposure to the selective P2Y2 receptor agonist UTP (Xu *et al.* 2003; Piskuric & Nurse, 2012; Tse *et al.* 2012; Zhang *et al.* 2012). The absence of cross-talk from type I to type II cells was confirmed by the lack of a $\Delta[Ca^{2+}]_i$ response in type II cells during perfusion with the depolarizing stimulus high K^+ (30 mM), which stimulates neurosecretion from type I cells in similar CB cultures (Buttigieg & Nurse, 2004; Livermore & Nurse, 2013). The '*n*' values reported in the text refer to the number of culture dishes sampled, where the Ca^{2+} response of each dish was taken as the mean peak $\Delta[Ca^{2+}]_i$ value obtained from 10–15 randomly chosen cells. Cells with basal $[Ca^{2+}]_i$ greater than 200 nM, or cells whose baseline exhibited continuous ramping during the experiment, were excluded from analyses. In voltage clamp experiments, solitary type II cells were first 'tentatively' identified by their elongated morphology, and subsequently confirmed by their characteristic electrophysiological profile, including the presence of activatable Panx-1 currents (Duchen *et al.* 1988; Zhang *et al.* 2012).

Angiotensin II induces a rise in intracellular Ca^{2+} in type II cells via AT_1 receptors: comparison with type I cells

As exemplified in Fig. 1*A*, perfusion of ∼2-day-old CB cultures with ANG II led to a dose-dependent increase in intracellular Ca^{2+} ($\Delta[Ca^{2+}]_i$) in type II cells, identified by the presence of a positive $\Delta[Ca^{2+}]_i$ response to UTP (100 μM), but not high K^+. In one experimental series, the majority of UTP-sensitive type II cells (401/537; ∼75%) were also sensitive to ANG II. A plot of the dose–response curve for ANG II *versus* $\Delta[Ca^{2+}]_i$ indicated an EC_{50} of approximately 8 nM, a value comparable to that previously reported for ANG II acting at AT_1 receptors in rat podocytes ($EC_{50} = 3$ nM; Henger *et al.* 1997). Repeated application of a high dose of ANG II (100 nM) tended to produce diminishing $\Delta[Ca^{2+}]_i$ responses in a given cell (Fig. 1*B*), probably due to receptor desensitization which is a well-known property of AT_1 receptors (Zhang *et al.* 1996; Guo *et al.* 2001). A histogram showing the time course of this desensitization phenomenon is shown in Fig. 1*D*.

Previous studies in rat CB using western blot, *in situ* hybridization, RT-PCR and immunohistochemical techniques revealed high expression of AT_1 receptors (AT_1Rs), localized predominantly to type I cells (Leung *et al.* 2000; Fung *et al.* 2001; Lam & Leung, 2002). It was therefore of interest to determine whether or not the ANG II-induced $\Delta[Ca^{2+}]_i$ responses in type II cells were also mediated by AT_1 receptors. First, we confirmed that ANG II elicited a rise in $[Ca^{2+}]_i$ in type I cells present in the same cultures (Fig. 2*A*). Notably, a comparison of the relative magnitude of the peak $\Delta[Ca^{2+}]_i$ evoked by the same dose of ANG II revealed that type II cells generated a much more robust Ca^{2+} response than type I cells (Fig. 2*B*). The mean $\Delta[Ca^{2+}]_i$ induced by 100 nM ANG II was ∼95 nM in type II cells compared to ∼32 nM for type I cells; the latter value was comparable to that previously reported for rat type I cells (∼20 nM; Fung *et al.* 2001). In a few cases, we confirmed that the type II cell

responses did not arise secondarily from ANG II-induced release of ATP from type I cells using the P2Y2R blocker suramin; the mean (±SEM) $\Delta[Ca^{2+}]_i$ response was 76.6 ± 12.8 nM for ANG II (100 nM), 59.5 ± 12.2 nM for ANG II plus 100 μM suramin, and 68.6 ± 12.4 nM for ANG II after washout of suramin ($n = 3$ dishes; $P > 0.05$).

The ANG II-induced $\Delta[Ca^{2+}]_i$ in type II cells was completely inhibited by the specific AT_1R blocker losartan (1 μM), and the effect was reversible (Fig. 2*C*); a scatter plot of $\Delta[Ca^{2+}]_i$ responses before, during and after losartan is shown in Fig. 2*E*. Losartan significantly reduced the proportion of ANG II-responsive type II cells by 95% (only 30/545 cells that initially responded to ANG II did so in the presence of losartan); also, the mean $\Delta[Ca^{2+}]_i$ response was reduced by 97% (mean $\Delta[Ca^{2+}]_i$ before and during losartan was 101 ± 9.3 nM *vs.* 3.1 ± 1.8 nM, $n = 10$ dishes; repeated measures ANOVA with Tukey's multiple comparison test *post hoc* test, $P < 0.05$). After wash-out of losartan there was an ~80% recovery of the original ANG II-evoked Ca^{2+} response. We also confirmed that the ANG II-induced response in type I cells was also inhibited by losartan (Fig. 2*C*), as previously reported (Fung *et al.* 2001). Taken together these data imply that functional AT_1Rs are expressed in both type I and type II cells of rat CB.

Angiotensin II-induced Ca^{2+} transients in type II cells originate mainly from intracellular stores

In general, ANG II–AT_1R signalling is mediated either via entry of extracellular Ca^{2+} through Ca^{2+} channels or activation of the phosphatidylinositol–inositol-1,4,5-trisphosphate (IP_3) pathway coupled to Ca^{2+} release from internal stores (Balla *et al.* 1991; Henger *et al.* 1997; Goette & Lendeckel, 2008; Schultz, 2011).

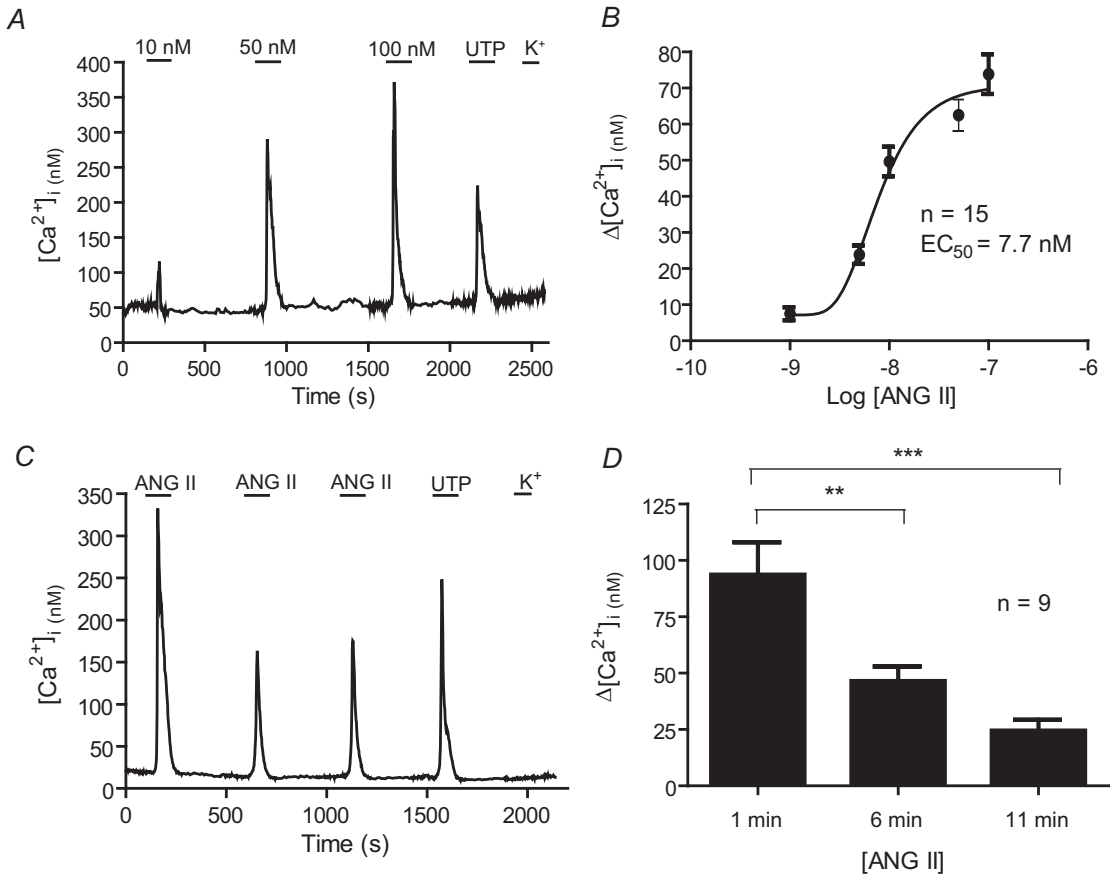

Figure 1. Effects of angiotensin II (ANG II) on intracellular calcium transients in type II cells
The effects of increasing doses of ANG II (10, 50, 100 nM) on intracellular Ca^{2+} concentration ($[Ca^{2+}]_i$) in a type II cell is shown in *A*; for type II cell identification note typical increase in Ca^{2+} ($\Delta[Ca^{2+}]_i$) to UTP (100 μM), but not high K^+ (30 mM). *B*, dose–response relation for ANG II-induced $\Delta[Ca^{2+}]_i$ in type II cells; a fit of the dose–response curve with the Hill equation yielded an $EC_{50} = 7.7$ nM ($n = 15$ dishes). *C*, decrease in $[Ca^{2+}]_i$ responses in type II cells with repeated exposures to 100 nM ANG II, attributable to receptor desensitization. *D*, time course of the reduction in $\Delta[Ca^{2+}]_i$ responses in type II cells after 1, 6 and 11 min exposure to 100 nM ANG II; $^{**}P < 0.01$; $^{***}P < 0.001$, repeated measures ANOVA with Tukey's multiple comparison test *post hoc* test.

To determine whether the ANG II-induced $\Delta[Ca^{2+}]_i$ in type II cells arose principally from entry of extracellular Ca^{2+}, we first monitored Ca^{2+} transients in nominally Ca^{2+}-free medium. As shown in Fig. 3*A*, Ca^{2+} transients evoked by 100 nM ANG II were not significantly altered in Ca^{2+}-free medium, consistent with a predominant release from intracellular stores; mean ± SEM $\Delta[Ca^{2+}]_i$ in calcium-free solution was 80.6 ± 15 nM, whereas the mean ± SEM in normal calcium was 105.0 ± 17 nM ($n = 9$ dishes; Mann–Whitney test, $P = 0.3$). In order to avoid

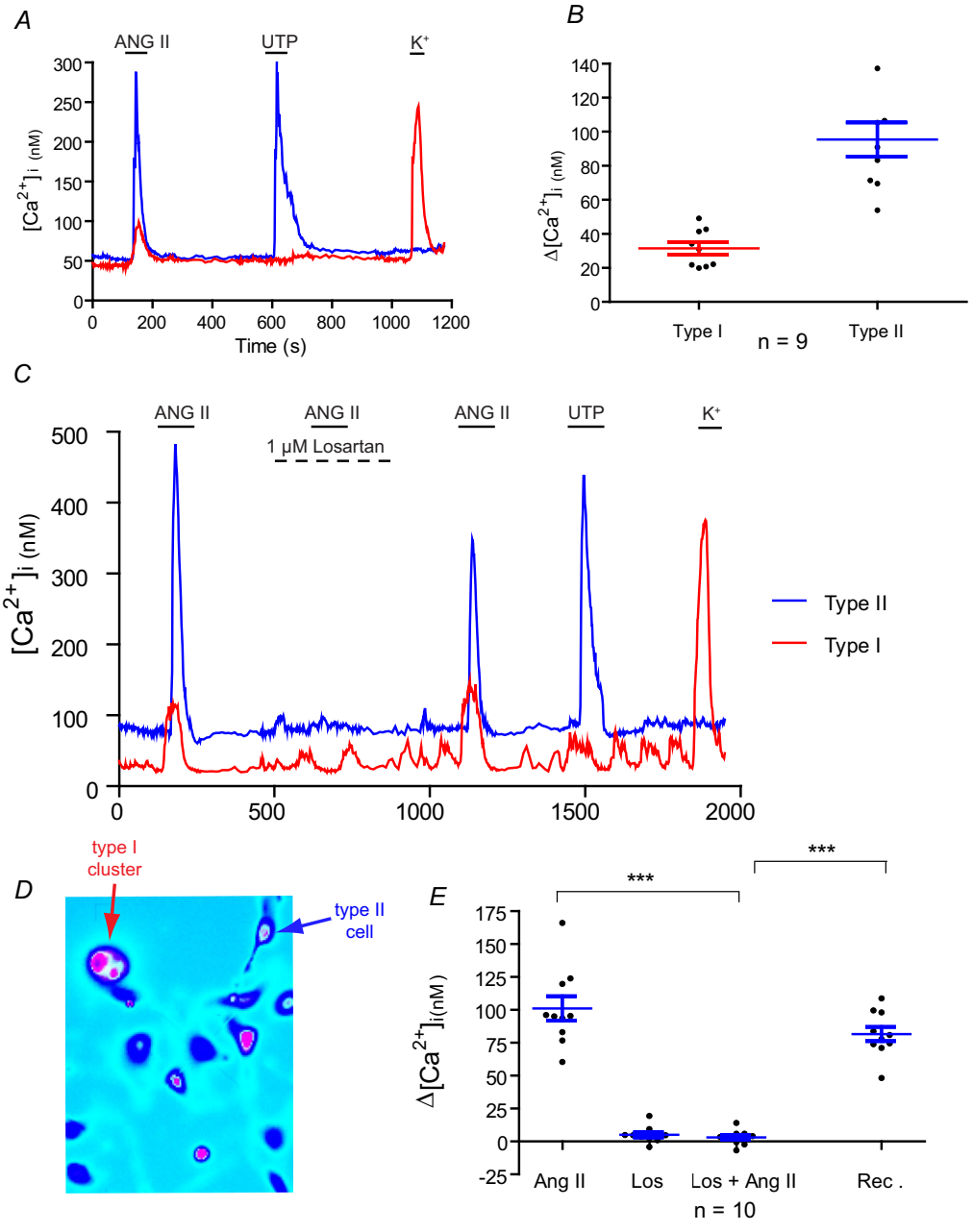

Figure 2. Comparison of the effects of angiotensin II (ANG II) in type II *versus* type I cells and role of AT_1 receptors
In *A*, ANG II (100 nM) causes a rise in intracellular Ca^{2+} concentration ($[Ca^{2+}]_i$) in both a type II cell and a type I cell in the same culture; note that the type II cell, which responds to UTP but not high K^+, elicits a more robust Ca^{2+} response than the type I cell, which responds to high K^+ but not UTP. Comparison of mean ± SEM $\Delta[Ca^{2+}]_i$ responses in type II *versus* type I cells after exposure to 100 nM ANG II is shown in *B* ($n = 9$ dishes; 10–15 cells sampled per dish). In *C*, the ANG II-induced rise in $[Ca^{2+}]_i$ is reversibly abolished by the selective AT_1 receptor blocker, losartan (1 μM), in both the type II cell and a type I cell within the cluster identified in *D*. Summary data from 10 dishes are shown in *E*. ***$P < 0.001$.

the effect of desensitization, the first ANG II-evoked Ca^{2+} responses were compared either in the presence or absence of extracellular Ca^{2+}. Figure 3*B* illustrates this comparison as a scatter plot of the ANG II-induced $\Delta[Ca^{2+}]_i$ in type II cells in normal (2 mM) and zero Ca^{2+} solutions. To confirm a major role for Ca^{2+} release from intracellular stores, we monitored Ca^{2+} transients in the presence of the store-depleting agent cyclopiazonic acid (CPA; 10 μM). As shown in Fig. 3*C* and *D*, the ANG II-induced $\Delta[Ca^{2+}]_i$ was markedly inhibited by CPA, suggesting that Ca^{2+} release from stores was a major contributor to ANG II–AT_1R signalling in type II cells; the mean ± SEM $\Delta[Ca^{2+}]_i$ in control *vs.* CPA-containing solutions was 88 ± 9.7 *vs.* 13.5 ± 2.0 nM; $n = 12$ dishes; Friedman test with Dunn's multiple comparison test, $P < 0.05$).

Angiotensin II-induced signalling activates pannexin-1 currents in type II cells

We next determined whether or not ANG II-induced signalling led to the activation of Panx-1 currents in type II cells, as previously demonstrated for ATP acting via P2Y2 receptors (Zhang *et al.* 2012). As exemplified in Fig. 4*A*, ANG II caused a dose-dependent activation of Panx-1 currents that arose with a variable delay. A plot of peak Panx-1 current density (pA/pF; at −60 mV holding potential) *vs.* ANG II concentration over the dose range 20–1000 nM is shown in Fig. 4*B*. Often, the ANG II-evoked Panx-1 current showed more than one plateau or multiple peaks (Figs 4*A* and 5*B*); in such cases the largest peak value seen in the inward current trace was used in constructing the dose–response curve. The variability in the delay of

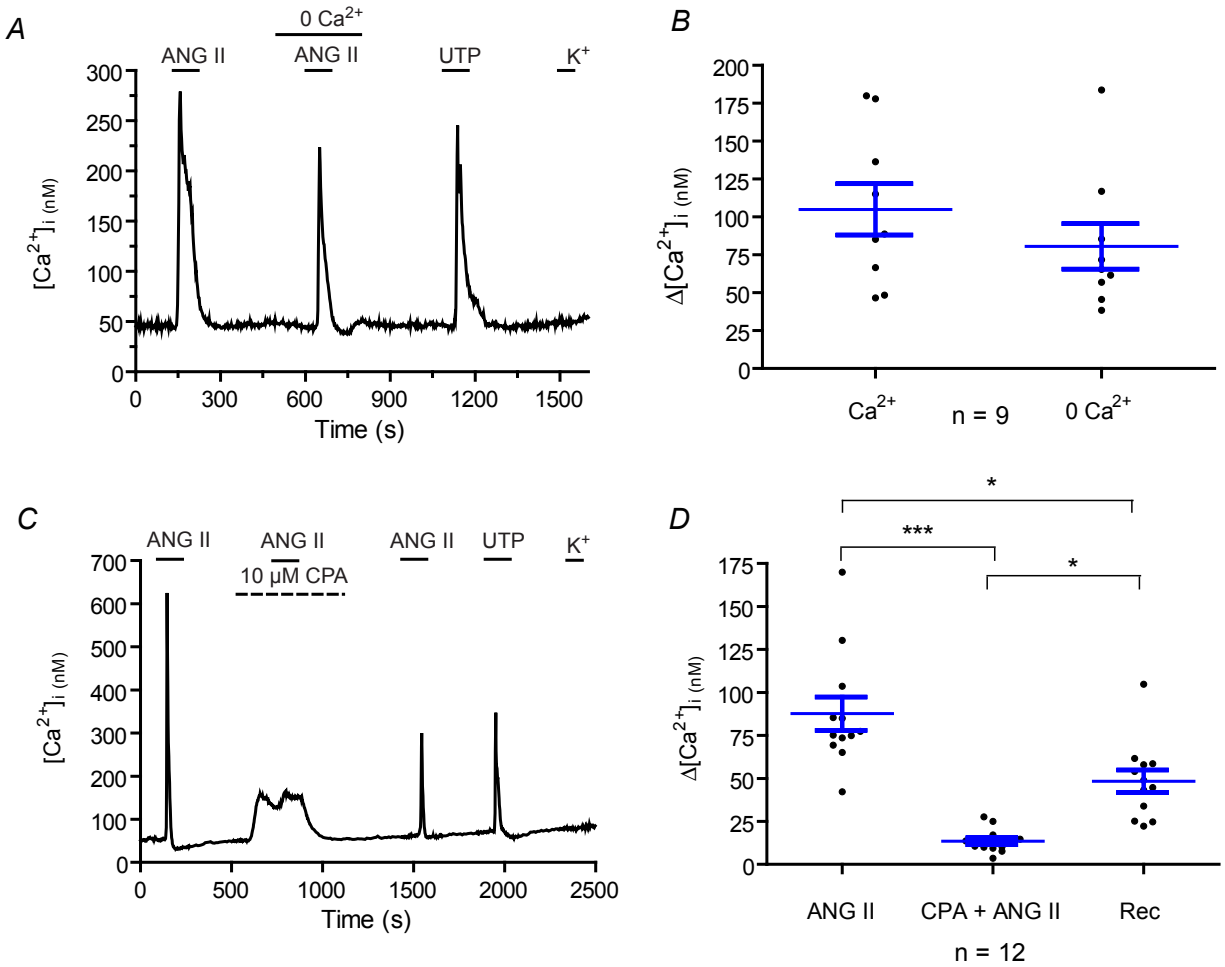

Figure 3. Role of intracellular stores in angiotensin II-induced rise in $[Ca^{2+}]_i$ in type II cells
In *A*, the ANG II-induced rise in $[Ca^{2+}]_i$ persists in solution containing nominally free extracellular Ca^{2+} (0 Ca^{2+}); summary data of mean ± SEM Ca^{2+} responses from 9 dishes are shown in *B*. In *C*, the ANG II-induced rise in $[Ca^{2+}]_i$ is inhibited by cyclopiazonic acid (CPA; 10 μM); note small Ca^{2+} response on exposing cells to CPA alone. Summary data of $\Delta[Ca^{2+}]_i$ from type II cells in 12 dishes before, during and after CPA are shown in *D*. *$P < 0.05$; ***$P < 0.001$.

current activation *versus* ANG II concentration is plotted in Fig. 4*C*, and is reminiscent of a similar observation noted during P2Y2R-induced activation of Panx-1 currents in these cells (Zhang *et al.* 2012). Panx-1 currents in type II cells could not be activated at a concentration of 10 nM ANG II or less (n = 10), at least within 100 s of exposure.

To confirm that the ANG II-activated current ($I_{ANG\ II}$) displayed the expected properties of Panx-1 currents we first measured the reversal potential (E_{rev}). In our

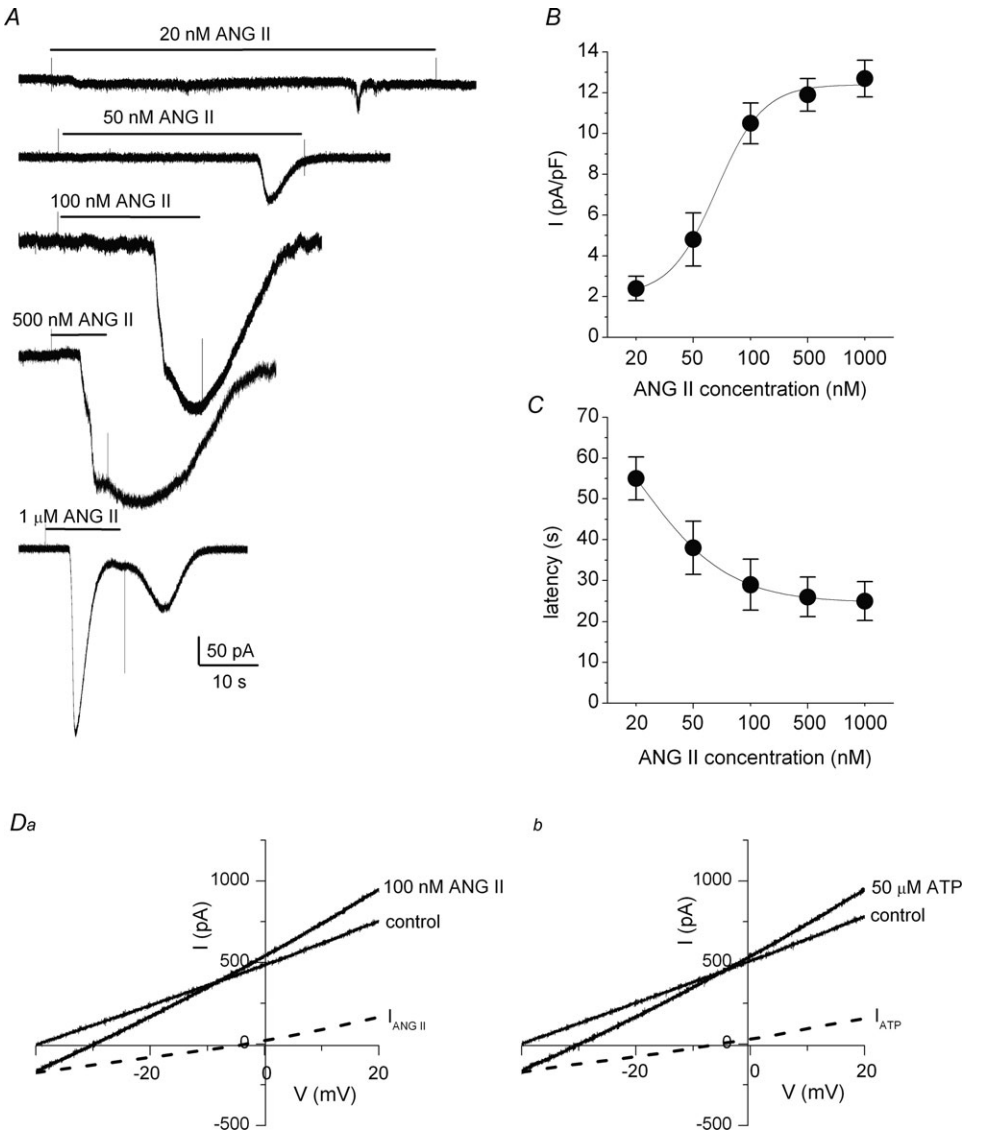

Figure 4. Dose dependence and reversal potential of ANG II-induced current in type II cells
In *A*, application of angiotensin II (ANG II) by a rapid perfusion system induced a dose-dependent inward current that arose with a variable latency; holding potential = −60 mV. The dose–response curve of peak current density (*I* (pA/pF)) *versus* ANG II concentration is shown in *B* (n = 5–7 cells); a fit of the dose–response curve with the Hill equation yielded an EC_{50} of 76 nM. A plot of latency of the peak current response *versus* ANG II concentration is shown in *C* for the same cells. In *Da*, an estimate of the reversal potential of the ANG II-induced current was obtained for a type II cell using a ramp protocol (holding potential −60 mV; ramp from −40 to +20 mV over 700 ms, repeated every 6 s) described in Methods; the dashed curve shows the $I_{ANG\ II}$ difference current, obtained by subtracting the current evoked in the presence of 100 nM ANG II from the control current, reversed at ∼ −6 mV for this cell. In *Db*, the same cell was tested in a similar way using ATP, which was previously shown to activate Panx-1 current in type II cells via P2Y2R (Zhang *et al.* 2012); the I_{ATP} difference current in *Db* showed a similar reversal potential to $I_{ANG\ II}$, as expected if both ligands activated the same target, i.e. Panx-1 channels. *Da* and *Db* are representative of 5 cells treated with this protocol.

previous study, P2Y2R stimulation activated Panx-1 current with a E_{rev} near ~0 mV (Zhang *et al.* 2012). Because of current run-down observed during repeated ANG II applications due to receptor desensitization (see below), as well as variability in response latency, we used a repeated ramp protocol to estimate E_{rev} of the ANG II difference current ($I_{ANG\,II}$) as described in Methods. As exemplified in Fig. 4*Da* for a type II cell exposed to 100 nM ANG II, E_{rev} of $I_{ANG\,II}$ was ~ −6 mV; the mean E_{rev} for a group of five cells was −5.7 ± 2.6 mV, consistent with the opening of non-selective ion channels. Indeed, when both ANG II and ATP were tested on the same cell, as exemplified in Fig. 4*Da* and *b*, E_{rev} was indistinguishable for the two agonists, even though each acted at its own distinct receptor; for ATP the mean E_{rev} was −3.2 ± 1.8 mV ($n = 5$).

Final validation that ANG II activated Panx-1 currents in type II cells was obtained using the selective blocker carbenoxolone (CBX) at low concentrations (5 μM), thought to block Panx-1 channels but not gap junctional channels (Barbe *et al.* 2006; Ma *et al.* 2009). As in our previous study using P2Y2R agonists (Zhang *et al.* 2012), the ANG II-induced inward current at −60 mV holding potential was reversibly abolished by 5 μM CBX (Fig. 5*A* and *C*; $n = 5$), consistent with Panx-1 channels as the current carrier.

Pannexin-1 current activation by angiotensin II is mediated via AT_1 receptors in type II cells

Given that AT_1R is the major ANG II receptor subtype expressed in the rat CB (Leung *et al.* 2000; Fung *et al.*

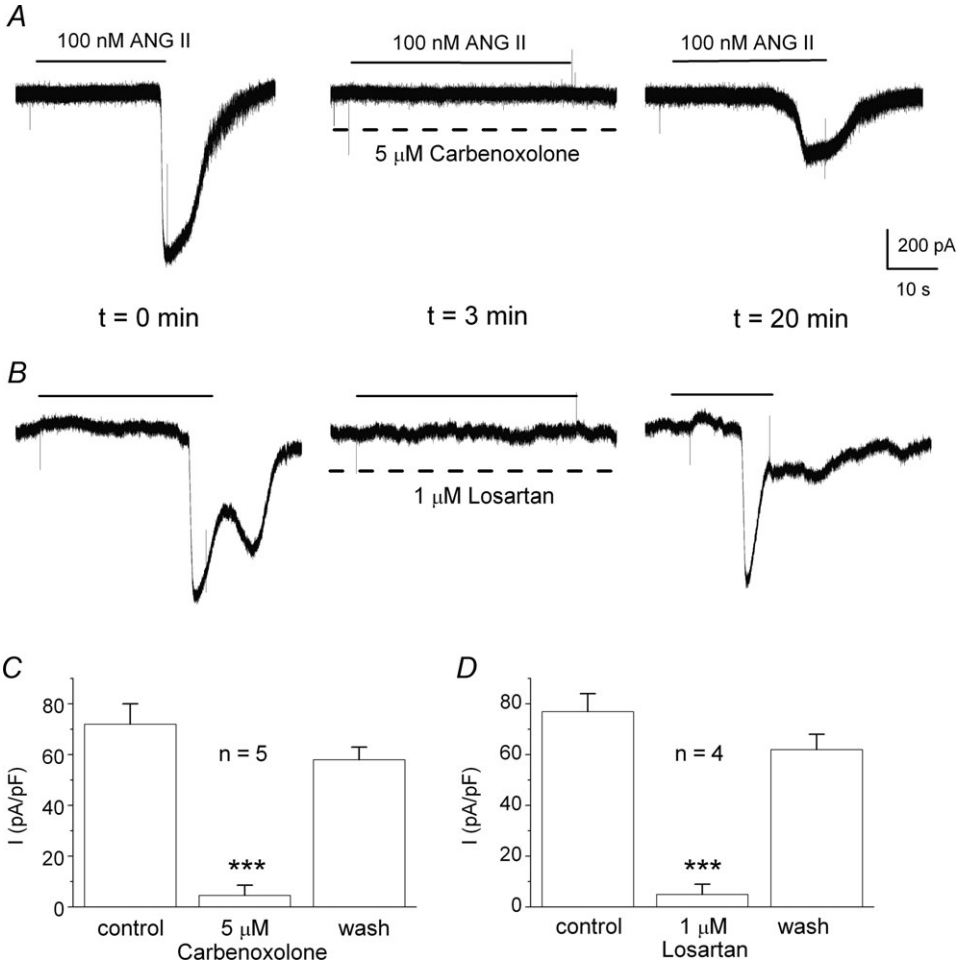

Figure 5. Blockade of angiotensin II-induced inward currents in type II cells by carbenoxolone and losartan
In *A*, the inward current elicited by 100 nM ANG II at −60 mV (holding potential) was reversibly inhibited in a type II cell by the Panx-1 channel blocker carbenoxolone (CBX; 5 μM); pooled current density (pA/pF) data for a group of 5 cells before, during and after CBX are summarized in *C*. In *B*, the ANG II-induced current was reversibly inhibited by the specific angiotensin AT_1 receptor blocker, losartan (1 μM); pooled current density (pA/pF) data for a group of 4 cells before, during and after losartan are summarized in *D*. ***$P < 0.001$.

2001; Lam & Leung, 2002), and that AT_1Rs mediated the ANG II-induced rise in $[Ca^{2+}]_i$ in type II cells (see above), we investigated whether Panx-1 current activation was also mediated via AT_1Rs using the selective blocker losartan (de Gasparo *et al.* 2000). As exemplified in Fig. 5*B*, the ANG II-induced Panx-1 current in type II cells was reversibly abolished by losartan (1 μM); a histogram of the ANG II-induced Panx-1 current density (pA/pF; at −60 mV holding potential) for a group of four cells before, during and after exposure to 1 μM losartan is shown in Fig. 5*D*.

Consistent with the well-known desensitization properties of the AT_1R (see above), repeated application of ANG II to the same cell routinely resulted in Panx-1 current run-down, as exemplified in Fig. 6*A*. The time course of decay of $I_{ANG\,II}$ current density (at −60 mV holding potential) during repeated applications of ANG II over a 20 min period is shown in Fig. 6*C*. This contrasts with the effect of ATP acting via P2Y2Rs on Panx-1 current which typically remained stable during repeated applications of ATP over the same time period (Fig. 6*B* and *C*). Current run-down was not due to 'inactivated' or non-functional Panx-1 channels because the current could be promptly restored (within 2 min), soon after run-down induced by high doses of ANG II (100 nM to 1 μM), by simply applying ATP to the same cell (e.g. Fig. 6*D*; $n = 4$ cells). Taken together, these data indicate that both the ANG II-induced rise in $[Ca^{2+}]_i$ and Panx-1 current activation are mediated via functional AT_1Rs expressed in type II cells.

Combined actions of angiotensin II and ATP lead to a synergistic activation of pannexin-1 current in type II cells

Over the course of this study it was routinely observed that solitary type II cells often responded to both ATP/UTP and ANG II with a rise in intracellular Ca^{2+} or activation of Panx-1 current. While ANG II in the picomolar range can produce physiological effects at AT_1Rs in the intact CB (Allen, 1998; Peng *et al.* 2011), relatively higher doses (≥20 nM) were required to activate Panx-1 current, at least within 100 s of application. Given that during CB chemoexcitation it is unlikely that ANG II will be acting alone, we wondered whether its actions might be complementary to those of other excitatory mediators such as ATP. Indeed, we found that doses of ANG II and ATP (below the EC_{50} and near the foot of their respective dose–response curves) interacted synergistically when applied to the same cell. First, as exemplified in Fig. 7*A*, when a near-threshold dose of ATP (10 μM) sufficient to activate the Panx-1 current was combined with a 'subthreshold' dose of ANG II (10 nM) that failed to do so in a given cell, there was a >1.5× potentiation of the ATP-evoked response ($n = 3$ cells). Second, whereas each of the doses 10 μM ATP and 20 nM ANG II activated a detectable Panx-1 current when applied separately to the same type II cell, the current was markedly potentiated when the same doses were applied together (Fig. 7*B*). A histogram showing mean Panx-1 current density (pA/pF) for a group of five cells exposed to 10 μM ATP and 20 nM ANG II separately, and then in combination, is shown in Fig. 7*C*. These data suggest the current response from the combined application was more-than-additive, and was ∼1.6× larger than the sum of the two separate applications ($P < 0.05$; Fig. 7*C*). Interestingly, during the combined application the latency of the current response was significantly shorter than the minimum observed for either ligand acting alone (Fig. 7*D*; $P < 0.01$).

Angiotensin II- and ATP-induced pannexin-1 current in type II cells requires a rise in intracellular Ca^{2+}

In oocyte expression systems, cytoplasmic Ca^{2+} in the micromolar range was sufficient to activate human Panx-1 channels (Locovei *et al.* 2006); however, the requirement for a rise in $[Ca^{2+}]_i$ has been questioned in another study (Ma *et al.* 2009). To test whether or not the rise in cytoplasmic Ca^{2+} elicited in type II cells by ANG II and ATP (Xu *et al.* 2003; Zhang *et al.* 2012) was necessary for activation of the Panx-1 current, we used the membrane-permeable Ca^{2+} chelator BAPTA-AM (1 μM). As exemplified in Fig. 8*A* and *B*, the Panx-1 current induced by either ANG II or ATP was reversibly inhibited by BAPTA; pooled data from cells exposed to ANG II or ATP are summarized in Fig. 8*C* and *D*, respectively. Taken together, these data support the notion that a rise in cytoplasmic Ca^{2+} is required for Panx-1 channel activation by both agonists.

Discussion

The presence of a locally generating, renin-independent, ANG II system was identified in the carotid body (CB) many years ago and has generated much interest and speculation about its physiological function (Lam & Leung, 2002; Schultz & Li, 2007; Peng *et al.* 2011; Schultz, 2011). The present study has highlighted a novel aspect of ANG II signalling in the rat CB involving sustentacular, glial-like type II cells. Prior to this study, the focus of ANG II actions was understandably centred on CB chemoreceptor type I cells, because they expressed functional AT_1 receptors (AT_1Rs), as well the biosynthetic machinery for ANG II synthesis (Allen, 1998; Fung *et al.* 2001; Lam & Leung, 2002; Schultz, 2011). However, we provide strong evidence that type II cells, which are normally found in intimate association with type I cells in the CB, are also likely to be an important target for the actions

of ANG II. In particular, we show that ANG II acting via losartan-sensitive AT_1Rs induces a robust increase in intracellular Ca^{2+} in isolated type II cells; this in turn leads to the activation of Panx-1 channels, which we recently showed act as conduits for ATP release from these cells (Zhang *et al.* 2012). We are unaware of any other studies demonstrating a link between ANG II signalling and the activation of Panx-1 channels; however, these channels are known to facilitate release of ATP as well as other chemical signals from a variety of cell types (MacVicar & Thompson, 2010; Sridharan *et al.* 2010). Previous immunohistochemical studies reported the presence of positive AT_1R-immunoreactivity in CB type I cells; however, these studies did not include tests for whether or not type II cells were also immuno-positive (Leung *et al.* 2000; Li *et al.* 2006). We did not attempt to co-localize AT_1R immunoreactivity with known type II cell markers because as many as six commercially available AT_1R antibodies have recently been found to be non-specific when tested on AT_1 knock-out animals (Benicky *et al.* 2012). We also confirmed the previous findings of Fung *et al.* (2001) indicating that ANG II stimulates a rise in intracellular Ca^{2+} in rat type I cells via AT_1Rs; however, these Ca^{2+} signals tended to be much smaller in magnitude than those recorded in type II cells. In the latter study, the source of the AT_1R-mediated rise in intracellular Ca^{2+} in rat type I cells was not identified (Fung *et al.* 2001). However, in rabbit type I cells ANG II has been reported to exert an excitatory

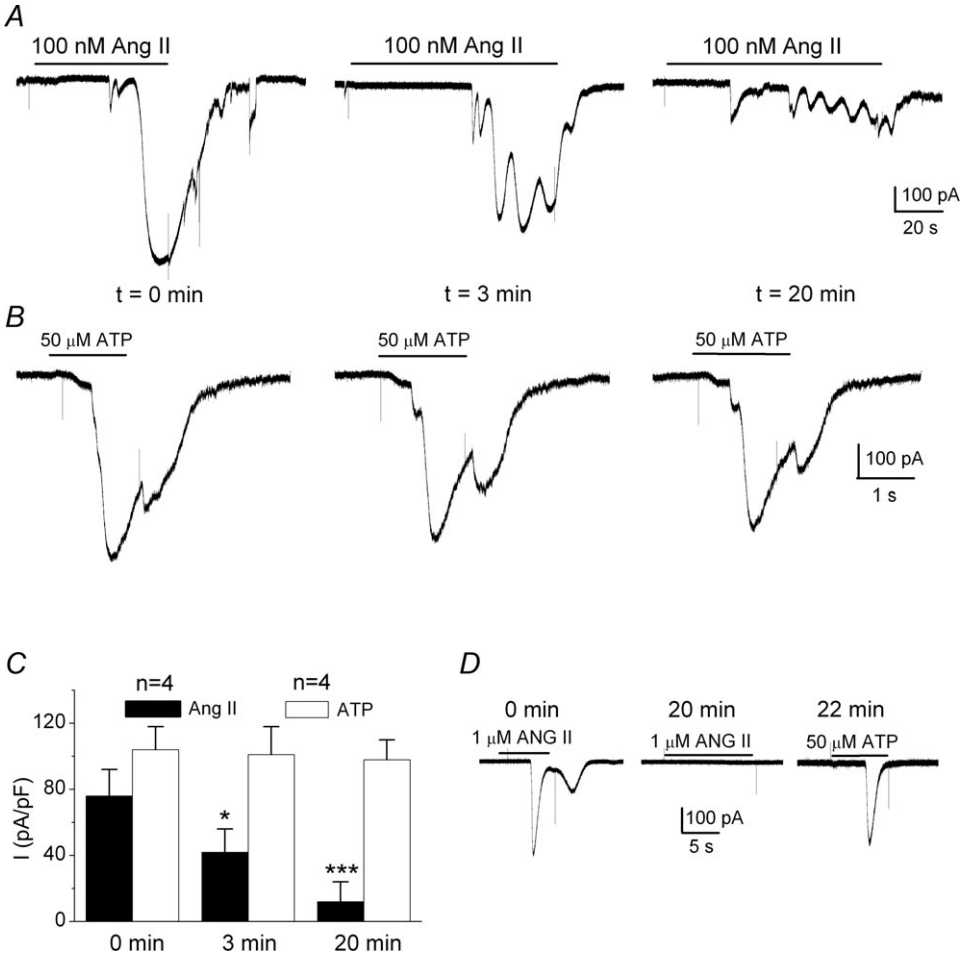

Figure 6. Comparison of angiotensin II- and ATP-induced Panx-1 current in type II cells during repeated agonist application
In *A*, repeated application of 100 nM ANG II to the same cell over a 20 min period ($t = 0$ min, left; $t = 3$ min, middle; $t = 20$ min, right) caused a progressive run-down in the peak current (at −60 mV holding potential); summary data from 4 cells are shown in *C* (filled columns). By contrast, when 50 μM ATP was used as the agonist, the current remained relatively stable over the same time period (*B* and *C*; open columns). Current run-down in *A* was attributable to desensitization of the AT_1 receptor, and not loss of Panx-1 channel function, because ATP could readily activate the Panx-1 current soon after (within 2 min) a test with ANG II failed to do so (*D*); test times with ANG II and ATP indicated above traces. Example in *D* was typical of $n = 4$ cells, exposed to 100 nM or 1 μM ANG II; $^*P < 0.05$; $^{***}P < 0.001$.

effect mediated via AT_1Rs and activation of NADPH oxidase, leading to inhibition of various K^+ channels, membrane depolarization and voltage-gated Ca^{2+} entry (Schultz, 2011). These data suggest that during AT_1R stimulation the source of the $[Ca^{2+}]_i$ rise in type I cells is extracellular, in contrast to type II cells where the source is intracellular (this study). Also, as discussed below, the ANG II–AT_1R signalling pathway in type II cells leads to the activation of pannexin–1, non-selective, ion channels. This contrasts with the inhibition of voltage-gated K^+ ($I_{K(V)}$) channels seen in type I cells (Schultz & Li, 2007; Schultz, 2011), which appear to lack pannexin-1 channel expression at least in the rat (Zhang *et al.* 2012).

Angiotensin II–AT_1R–pannexin-1 signal transduction pathway in type II cells

Ratiometric fura-2 imaging experiments revealed that ANG II elicited a rise in intracellular Ca^{2+} ($\Delta[Ca^{2+}]_i$) in type II cells that persisted in Ca^{2+}-free medium, but was sensitive to intracellular store depletion with cyclopiazonic acid. The principal ANG II receptor subtype involved was the AT_1R because the $\Delta[Ca^{2+}]_i$ responses were reversibly abolished by the specific AT_1R blocker losartan (de Gasparo *et al.* 2000). These observations suggest ANG II–AT_1R signalling in type II cells occurs mainly via the ubiquitous G-protein-coupled, phosphatidylinositol–IP_3 pathway, whereby activation of

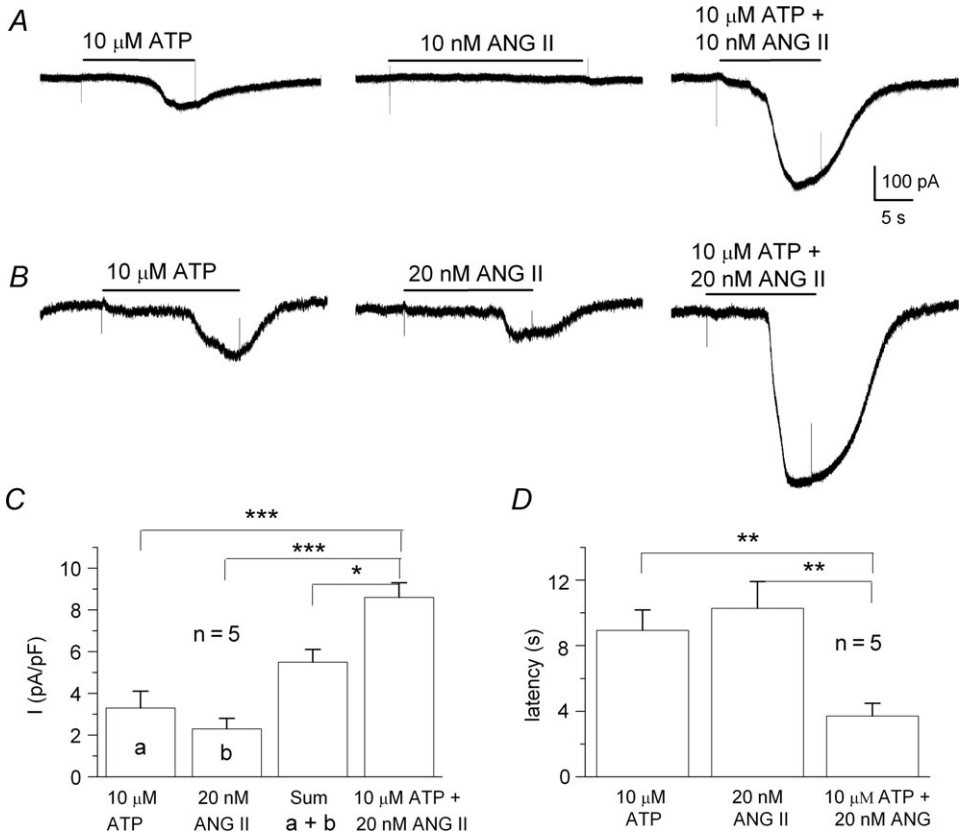

Figure 7. Synergistic interaction between ATP and angiotensin II on Panx-1 current activation in type II cells
In *A*, a low dose of ATP (10 μM; left trace) activated the Panx-1 current whereas a 'subthreshold' dose of ANG II (10 nM; middle trace) failed to do so in the same cell; when the two stimuli were combined the current was markedly potentiated relative to that seen with ATP alone ($n = 3$). In *B*, both ATP (10 μM; left trace) and ANG II (20 nM; middle trace), at doses below their respective EC_{50} values of 34 μM (Zhang *et al.* 2012) and 76 nM (this study), elicited a detectable Panx-1 current in the same type II cell when applied separately; however, when applied together there was a marked potentiation in the magnitude of the response, as well as a shortening of the response latency (right trace). Summary data in *C* show that the current density (pA/pF at −60 mV holding potential) elicited when the two agonists were applied together (right column) exceeded the sum of the separate individual responses (sum of column a + column b) by a factor of ~×1.6 ($P < 0.05$), indicating a synergistic interaction ($n = 5$ cells). In *D*, response latency during combined application was significantly shorter than that seen during separate application of either agonist. Note in *B* and *D*, the average latency during ANG II application appeared much shorter (~9 s) when the agonist was applied after prior activation or 'priming' of the Panx-1 current by ATP (compare with Fig. 4, where latency was ~55 s for 20 nM ANG II, without prior ATP exposure). *$P < 0.05$; **$P < 0.01$; ***$P < 0.001$.

phospholipase C leads to the generation of IP_3 which in turn triggers Ca^{2+} release from the endoplasmic reticulum (Guo *et al.* 2001). The AT_1 receptors are known to undergo rapid internalization and desensitization upon repeated stimulation (Zhang *et al.* 1996; Guo *et al.* 2001), and this property was the likely basis for the progressive decrease in $\Delta[Ca^{2+}]_i$ responses seen with repetitive ANG II applications. The estimated EC_{50} for the ANG II–AT_1R-evoked Ca^{2+} responses was ~8 nM, a value comparable to that seen in other cell types with this technique (Henger *et al.* 1997); in competitive binding studies, the IC_{50} for ANG II at AT_1Rs was reported to be ~8 nM (Bosnyak *et al.* 2011).

Perforated-patch, whole-cell recordings from type II cells revealed that ANG II caused a dose-dependent activation of Panx-1 currents with a reversal potential near 0 mV, consistent with the opening of non-selective ion channels. As expected for the involvement of AT_1Rs, these currents were reversibly blocked by losartan (1 μM). Panx-1 current run-down was commonly observed during repeated ANG II applications, probably because of AT_1R desensitization (see above); however, for reasons that are presently unclear current run-down was not obvious immediately after recovery from AT_1R blockade by losartan. Also, because the current could be robustly restored immediately after ANG II-induced run-down by simply activating a different (ATP–P2Y2R) signalling pathway, loss of Panx-1 channel function could not account for the run-down. The latency of ANG II-induced Panx-1 current in 'solitary' type II cells was quite variable, typically >25 s, and depended on agonist concentration. During AT_1R signal transduction cascades, the ANG II-induced signal can arise with latencies that vary from seconds in the case of phospholipase C–IP_3-mediated release of Ca^{2+} from stores, to minutes in cases where other downstream signals (e.g. mitogen-activated protein kinase) are activated (Guo *et al.* 2001). In our previous studies using ATP (10–250 μM) to stimulate P2Y2Rs, the latency of Panx-current varied typically between 6 and 14 s for 'solitary' type II cells; by contrast, for type II cells present within chemoreceptor clusters, the latency was much shorter (<3 s) (Zhang *et al.* 2012). In the present study, the experiments were done on 'solitary' type II cells where coupling within the signalling pathway was probably less efficient than in cell clusters, perhaps contributing to the

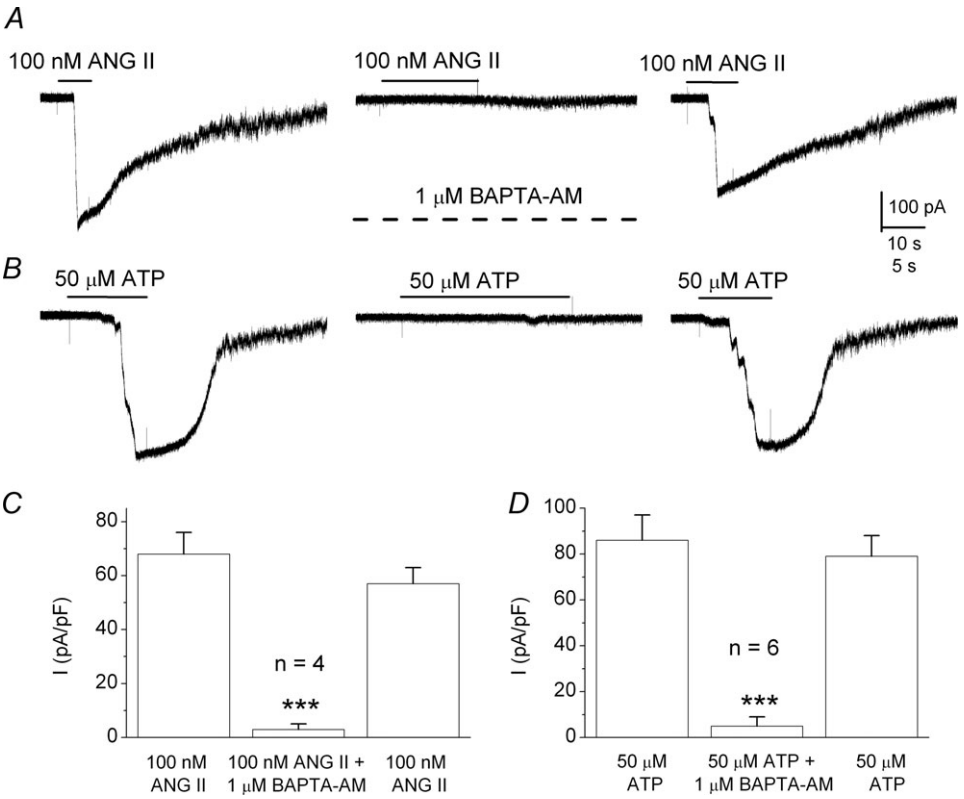

Figure 8. Chelating intracellular Ca^{2+} in type II cells with BAPTA prevents Panx-1 current activation by angiotensin II and ATP
In *A*, the ANG II-induced Panx-1 current was almost completely and reversibly inhibited during incubation with the membrane-permeable Ca^{2+} chelator BAPTA-AM (1 μM; middle trace). Similarly in *B*, the same result was obtained when ATP was used as the agonist. Summary data in *C* and *D* show the reversible inhibition of the Panx-1 current evoked by ANG II and ATP, respectively, when BAPTA-AM was present ($n = 4$ in *C*, and 6 in *D*); ***$P < 0.001$.

longer latencies. An interesting observation was that the latency of Panx-1 current activation by ANG II in 'solitary' type II cells appeared consistently shorter (<12 s) if the cells were first 'primed' by exposure to a P2Y2R agonist such as ATP. Further studies are required to clarify the underlying mechanism.

Physiological significance and clinical relevance

Using immunofluorescence, we previously demonstrated that Panx-1 channels are expressed in glial fibrillary acidic protein (GFAP)-positive type II cells in tissue sections of rat carotid body (CB) *in situ*, and in cultured dissociated CB cells (Zhang *et al.* 2012). Moreover, we showed that when these channels were activated in isolated type II cells using the P2Y2R agonist UTP, they acted as conduits for release of ATP, a key CB excitatory neurotransmitter (Nurse, 2010; Nurse & Piskuric, 2012; Zhang *et al.* 2012). In light of these findings, a plausible physiological role of ANG II signalling in type II cells is to stimulate Panx-1 channel opening and consequently ATP release, which could serve as a boost for CB excitation. The EC_{50} for ANG II as determined by Panx-1 current activation was ~76 nM, a value ~9× higher than that observed using Ca^{2+} imaging. In fact, Panx-1 currents were not detectable (at least with a latency <100 s) at 10 nM ANG II which is near the EC_{50} value based on intracellular Ca^{2+} measurements. These data suggest that a threshold level of intracellular Ca^{2+} may need to be reached for Panx-1 channel activation, or some other lower affinity process needs to be activated in parallel with the rise in Ca^{2+}, or combinations of these. It is arguable whether an increase in intracellular Ca^{2+} is a general pre-requisite for Panx-1 channel activation in different cell types (Locovei *et al.* 2006; Ma *et al.* 2009). However, in the present study the necessity for a rise in intracellular Ca^{2+} was demonstrated in experiments where Panx-1 currents were almost completely and reversibly blocked in the presence of the membrane-permeable Ca^{2+} chelator, BAPTA-AM (1 μM). Whether intracellular Ca^{2+} acts by binding directly to the Panx-1 channel in type II cells, or via some other (e.g. PKC) pathway, remains to be determined. Nonetheless, we cannot rule out the possibility that additional converging signalling pathways, for example activation of Src family kinases (Weilinger *et al.* 2012), are required for Panx-1 current activation.

The role of the local ANG II-generating system in normal CB function remains unclear. However, there are several pathophysiological conditions where upregulation of this local system occurs. These include conditions where animals are exposed to chronic or intermittent hypoxia (Leung *et al.* 2000; Lam & Leung, 2003; Lam *et al.* 2014), and in patients or animal models experiencing chronic heart failure (CHF) (Schultz & Li, 2007; Schultz, 2011). After exposure to chronic hypoxia, AT_1R mRNA and protein expression increases in the rat CB and there is enhanced AT_1R-mediated excitation of CB afferent activity (Leung *et al.* 2000). In the case of chronic intermittent hypoxia (CIH), a condition associated with sleep-disordered breathing, there is increased angiotensinogen, AT_1R mRNA and AT_1R protein expression in the CB, as well as increased type I cell Ca^{2+} responses to exogenous ANG II (Lam *et al.* 2014). In CHF rabbits, but not sham controls, pharmacological inhibition of AT_1R decreases CB chemoreceptor discharge to hypoxia, in association with increased hypoxic sensitivity of type I cells (Li *et al.* 2006; Schultz & Li, 2007; Schultz, 2011). In light of the accompanying increased local CB and systemic levels of ANG II in CHF (Schultz, 2011), it is plausible that ANG II-AT_1R signalling via type II cells may contribute to sensitization of CB sensory discharge via Ca^{2+}-dependent activation of Panx-1 channels and release of ATP. Indeed, this ATP release from type II cells may be further facilitated by the observed synergistic interactions between P2Y2R and AT_1R signal transduction pathways. In particular, we found that when low doses ($<EC_{50}$) of ANG II and ATP were applied to the same type II cell there was a synergistic enhancement of Panx-1 currents, which would be expected to cause further augmentation of ATP release and sensitization of CB function. In CHF, this increased CB sensitization appears maladaptive as it serves to exacerbate the tonic sympathetic hyperactivity associated with the disease progression (Schultz & Li, 2007; Schultz, 2011).

In conclusion, the present study has revealed a novel ANG II–AT_1R signalling pathway in glial-like type II cells of the rat carotid body leading to activation of Panx-1 channels, which act as conduits for release of ATP (Nurse & Piskuric, 2012; Nurse, 2014). Given that ATP is a key excitatory CB neurotransmitter, we propose that activation of this signalling pathway has the potential to contribute to CB excitation. This is especially likely to occur in pathophysiological conditions of exaggerated CB excitation such as chronic heart failure and sleep-disordered breathing, where components of the local ANG II–AT_1R system are upregulated (Lam *et al.* 2004; Schultz, 2011; Kumar & Prabhakar, 2012; Lam *et al.* 2014).

References

Allen AM (1998). Angiotensin AT_1 receptor-mediated excitation of rat carotid body chemoreceptor afferent activity. *J Physiol* **510**, 773–781.

Balla T, Baukal AJ, Eng S & Catt KJ (1991). Angiotensin II receptor subtypes and biological responses in the adrenal cortex and medulla. *Mol Pharmacol* **40**, 401–406.

Barbe MT, Monyer H & Bruzzone R (2006). Cell-cell communication beyond connexins: the pannexin channels. *Physiology (Bethesda)* **21**, 103–114.

Benicky J, Hafko R, Sanchez-Lemus E, Aguilera G & Saavedra JM (2012). Six commercially available angiotensin II AT_1 receptor antibodies are non-specific. *Cell Mol Neurobiol* **32**, 1353–1365.

Bosnyak S, Jones ES, Christopoulos A, Aguilar MI, Thomas WG & Widdop RE (2011). Relative affinity of angiotensin peptides and novel ligands at AT_1 and AT_2 receptors. *Clin Sci (Lond)* **121**, 297–303.

Buttigieg J & Nurse CA (2004). Detection of hypoxia-evoked ATP release from chemoreceptor cells of the rat carotid body. *Biochem Biophys Res Commun* **322**, 82–87.

de Gasparo M, Catt KJ, Inagami T, Wright JW & Unger T (2000). International Union of Pharmacology. XXIII. The angiotensin II receptors. *Pharmacol Rev* **52**, 415–472.

Drummond GB (2009). Reporting ethical matters in *The Journal of Physiology*: standards and advice. *J Physiol* **587**, 713–719.

Duchen MR, Caddy KW, Kirby GC, Patterson DL, Ponte J & Biscoe TJ (1988). Biophysical studies of the cellular elements of the rabbit carotid body. *Neuroscience* **26**, 291–311.

Fung ML, Lam SY, Chen Y, Dong X & Leung PS (2001). Functional expression of angiotensin II receptors in type-I cells of the rat carotid body. *Pflugers Arch* **441**, 474–480.

Goette A & Lendeckel U (2008). Electrophysiological effects of angiotensin II. Part I: signal transduction and basic electrophysiological mechanisms. *Europace* **10**, 238–241.

Grynkiewicz G, Poenie M & Tsien RY (1985). A new generation of Ca^{2+} indicators with greatly improved fluorescence properties. *J Biol Chem* **260**, 3440–3450.

Guo DF, Sun YL, Hamet P & Inagami T (2001). The angiotensin II type 1 receptor and receptor-associated proteins. *Cell Res* **11**, 165–180.

Henger A, Huber T, Fischer KG, Nitschke R, Mundel P, Schollmeyer P, Greger R & Pavenstadt H (1997). Angiotensin II increases the cytosolic calcium activity in rat podocytes in culture. *Kidney Int* **52**, 687–693.

Kumar P & Prabhakar NR (2012). Peripheral chemoreceptors: function and plasticity of the carotid body. *Compr Physiol* **2**, 141–219.

Lam SY, Fung ML & Leung PS (2004). Regulation of the angiotensin-converting enzyme activity by a time-course hypoxia in the carotid body. *J Appl Physiol (1985)* **96**, 809–813.

Lam SY & Leung PS (2002). A locally generated angiotensin system in rat carotid body. *Regul Pept* **107**, 97–103.

Lam SY & Leung PS (2003). Chronic hypoxia activates a local angiotensin-generating system in rat carotid body. *Mol Cell Endocrinol* **203**, 147–153.

Lam SY, Liu Y, Ng KM, Liong EC, Tipoe GL, Leung PS & Fung ML (2014). Upregulation of a local renin-angiotensin system in the rat carotid body during chronic intermittent hypoxia. *Exp Physiol* **99**, 220–231.

Leung PS, Lam SY & Fung ML (2000). Chronic hypoxia upregulates the expression and function of AT_1 receptor in rat carotid body. *J Endocrinol* **167**, 517–524.

Li YL, Xia XH, Zheng H, Gao L, Li YF, Liu D, Patel KP, Wang W & Schultz HD (2006). Angiotensin II enhances carotid body chemoreflex control of sympathetic outflow in chronic heart failure rabbits. *Cardiovasc Res* **71**, 129–138.

Livermore S & Nurse CA (2013). Enhanced adenosine A_{2b} receptor signaling facilitates stimulus-induced catecholamine secretion in chronically hypoxic carotid body type I cells. *Am J Physiol Cell Physiol* **305**, C739–C750.

Locovei S, Wang J & Dahl G (2006). Activation of pannexin 1 channels by ATP through P2Y receptors and by cytoplasmic calcium. *FEBS Lett* **580**, 239–244.

Ma W, Hui H, Pelegrin P & Surprenant A (2009). Pharmacological characterization of pannexin-1 currents expressed in mammalian cells. *J Pharmacol Exp Ther* **328**, 409–418.

MacVicar BA & Thompson RJ (2010). Non-junction functions of pannexin-1 channels. *Trends Neurosci* **33**, 93–102.

Marshall JM (1994). Peripheral chemoreceptors and cardiovascular regulation. *Physiol Rev* **74**, 543–594.

Nurse CA (2010). Neurotransmitter and neuromodulatory mechanisms at peripheral arterial chemoreceptors. *Exp Physiol* **95**, 657–667.

Nurse CA (2014). Synaptic and paracrine mechanisms at carotid body arterial chemoreceptors. *J Physiol* **592**, 3419–3426.

Nurse CA & Piskuric NA (2012). Signal processing at mammalian carotid body chemoreceptors. *Semin Cell Dev Biol* **24**, 22–30.

Ohtake PJ & Jennings DB (1993). Angiotensin II stimulates respiration in awake dogs and antagonizes baroreceptor inhibition. *Respir Physiol* **91**, 335–351.

Peng YJ, Raghuraman G, Khan SA, Kumar GK & Prabhakar NR (2011). Angiotensin II evokes sensory long-term facilitation of the carotid body via NADPH oxidase. *J Appl Physiol (1985)* **111**, 964–970.

Piskuric NA & Nurse CA (2012). Effects of chemostimuli on $[Ca^{2+}]_i$ responses of rat aortic body type I cells and endogenous local neurons: comparison with carotid body cells. *J Physiol* **590**, 2121–2135.

Schultz HD (2011). Angiotensin and carotid body chemoreception in heart failure. *Curr Opin Pharmacol* **11**, 144–149.

Schultz HD & Li YL (2007). Carotid body function in heart failure. *Respir Physiol Neurobiol* **157**, 171–185.

Sridharan M, Adderley SP, Bowles EA, Egan TM, Stephenson AH, Ellsworth ML & Sprague RS (2010). Pannexin 1 is the conduit for low oxygen tension-induced ATP release from human erythrocytes. *Am J Physiol Heart Circ Physiol* **299**, H1146–H1152.

Tse A, Yan L, Lee AK & Tse FW (2012). Autocrine and paracrine actions of ATP in rat carotid body. *Can J Physiol Pharmacol* **90**, 705–711.

Weilinger NL, Tang PL & Thompson RJ (2012). Anoxia-induced NMDA receptor activation opens pannexin channels via Src family kinases. *J Neurosci* **32**, 12579–12588.

Xu J, Tse FW & Tse A (2003). ATP triggers intracellular Ca^{2+} release in type II cells of the rat carotid body. *J Physiol* **549**, 739–747.

Zakheim RM, Molteni A, Mattioli L & Park M (1976). Plasma angiotensin II levels in hypoxic and hypovolemic stress in unanesthetized rabbits. *J Appl Physiol* **41**, 462–465.
Zhang M, Piskuric NA, Vollmer C & Nurse CA (2012). P2Y2 receptor activation opens pannexin-1 channels in rat carotid body type II cells: potential role in amplifying the neurotransmitter ATP. *J Physiol* **590**, 4335–4350.
Zhang M, Turnbaugh D, Cofie D, Dogan S, Koshida H, Fugate R & Kem DC (1996). Protein kinase C modulation of cardiomyocyte angiotensin II and vasopressin receptor desensitization. *Hypertension* **27**, 269–275.
Zhang M, Zhong H, Vollmer C & Nurse CA (2000). Co-release of ATP and ACh mediates hypoxic signalling at rat carotid body chemoreceptors. *J Physiol* **525**, 143–158.
Zhong H, Zhang M & Nurse CA (1997). Synapse formation and hypoxic signalling in co-cultures of rat petrosal neurones and carotid body type 1 cells. *J Physiol* **503**, 599–612.

Additional information

Competing interests

None to declare.

Author contributions

S.M. initiated the study, prepared the cultures, carried out all the Ca^{2+} imaging experiments and data analysis, and helped prepare the figures. M.Z. performed all the electrophysiological experiments, analysed the data, and helped prepare the figures. C.A.N. was involved in the planning and designing of all the experiments, helped to interpret the data, and wrote the first draft of the manuscript. All authors approved the final version of this manuscript.

Funding

This work was supported by a Discovery grant from the Natural Sciences and Engineering Research Council of Canada (NSERC) to C.A.N. S.M. currently holds a CIHR/NSERC CGS-M graduate scholarship award.

Acknowledgements

We thank Cathy Vollmer and Dr Nikol Piskuric for their assistance.